

PCA and Health Indicators: Predicting Machine Failures Through Resistance Analysis

Ayu Dian Hartati^{1*}, Katherin Indriawati², Simion Sitepu³

^{1,2}Department of Engineering Physics, Industrial Technology and Systems Engineering, Institut Teknologi Sepuluh Nopember, Indonesia

³Utility Engineering Reliability and Maintenance System Department, PT Vale Indonesia, Soroako, Indonesia

¹ayudianhartati@gmail.com*; ²kindriawati@gmail.com; ³simion.sitepu@vale.com

*corresponding author

ABSTRACT

Predictive maintenance is crucial for ensuring industrial equipment's reliability and operational efficiency. This research aims to develop accurate health indicators to monitor real-time equipment conditions based on current signals. The methodology involves several key stages: collection of degradation data in current signals, data processing and mining, analysis using Principal Component Analysis (PCA), and development of health indicators. This study presents a comprehensive approach to converting raw degradation data into meaningful health indicators for effective engine prognostics and health management (PHM). Leveraging current signal data, we apply data mining and processing techniques to extract statistically significant features, including Standard Deviation, Peak to Peak, Root Mean Square (RMS), Crest Factor, Impulse Factor, Margin Factor, and Kurtosis. PCA is then used to reduce the dimensionality of the processed data, highlighting the principal components that capture the most significant variance indicating the machine's health. The resulting health indicators, derived from PCA, show a clear correlation between changes in additional load and increasing trends of PCA components and health indicators, thus validating the effectiveness of this approach in monitoring and predicting machine conditions. This methodology provides a robust real-time machine health assessment framework, facilitating timely maintenance and reducing the risk of unexpected failures. The results show that increasing resistance over time (t) leads to improved health indicators in a nonlinear manner, providing valuable insights for timely intervention before critical failure occurs. This analysis demonstrates a strong correlation between daily incremental resistance changes and machine condition as monitored by PCA and health indicators. Consistent upward trends in PCA scores and health indicators validate the effectiveness of this technique in tracking engine health under varying resistance conditions.

Keywords : Three Phase Synchronous Machine; Feature Extraction; Time-domain Analysis; PCA; Health Indicator; Resistance.

This is an open-access article under the [CC-BY-SA](https://creativecommons.org/licenses/by-sa/4.0/) license.



Article History

Received : June, 26th 2024

Accepted : Aug, 16th 2024

Published : Nov, 30th 2024

I. INTRODUCTION

Prognostics and health management (PHM) effectively regulates equipment use and ensures reliability. It is also a computing-based paradigm encompassing physical knowledge, information, and data [1][2]. Monitoring machine conditions and assessing performance degradation involves a crucial step: creating appropriate health indicators (HIs) [3]. Modern industrial systems often show HIs degradation over long-term operation. When an HI reaches the failure threshold during operation, the system may cause damage to property and harm to individuals [4]. By predicting failures before they occur, maintenance can be scheduled at convenient and cost-effective times, reducing downtime and minimizing the risk of unplanned outages.

Since appropriate HIs appropriately portray a system's health condition, they are essential to a non-end-to-end approach [5][6]. If the system experiences large fluctuations, understanding its current health status becomes challenging for individuals. HIs also significantly increase the difficulty of predicting the remaining useful life (RUL) with degradation models. Consequently, appropriate HI assistance is necessary to comprehend health status and facilitate accurate RUL predictions [7]. The HI research is intriguing because it addresses two main issues [8]: determining whether the built HI is helpful for RUL prediction and gleaning valuable information from monitoring data that may show a decline. Because of the nature of raw monitoring data, the first issue frequently includes complicated systems. Because of the inherent complexities of the underlying physics, intelligent features must be used to record health information in complex systems like bearings, machine tools, and turbofan engines. Several statistically based feature extraction techniques have been put forth for complex systems, including temporal domain-based techniques. [9], frequency-domain-based [10], time-frequency-domain-based [11], and other advanced approaches [12].

Regarding the second problem, various criteria, including readability, processability, and monotonicity, have been put forth to assess if an HI is appropriate for RUL prediction [13]. HIs are based on statistics and signal processing, offering clear physical interpretation and ease of calculation. They are usually derived from machine degradation data's time, frequency, or time-frequency domains. As two typical HIs statistics, root mean square (RMS) and Kurtosis have been widely applied for machine condition

management (MCM) in the industrial sector. RMS (Root Mean Square) can indicate trends in machine degradation based on energy measures, but it is less effective at detecting early signs of errors. On the other hand, Kurtosis, which assesses the transient impulses of a corrupted signal, is more sensitive to early mistakes. However, it does not consistently characterize the degradation process of the machine [14].

This research aims to develop health indicators based on current signals using data analysis techniques and Principal Component Analysis (PCA). These indicators will enable real-time monitoring of equipment conditions and aid in the early detection of damage. This research focuses on collecting and processing degradation data from current signals. The data processing and analysis methods employed include data mining and PCA, designed to simplify the data and highlight important features. This article is structured as follows: The first section reviews relevant literature. The second section outlines the methodology employed in this research. The third section presents the data analysis findings and health indicators' development. Finally, the last section offers the conclusions.

II. METHOD

As illustrated in Fig. 1, two online steps are proposed: feature extraction and classification. The rest of this section will provide a detailed explanation of these steps. The process flow diagram illustrated in Fig.1 outlines a comprehensive approach to monitoring and assessing system health using degradation data and flow signals. This method involves several key stages, starting with collecting degradation data, which forms the basis for subsequent analysis. Degradation data, particularly current signals, are meticulously collected and processed to extract meaningful patterns and trends. After processing the initial data, Principal Component Analysis (PCA) is applied. PCA is a statistical method that converts the processed data into a set of orthogonal components, which reduces dimensionality while preserving the most significant features. This step is crucial to simplifying the data, highlighting key variables contributing to system degradation, and facilitating more effective monitoring. Finally, the filtered data is used to develop health indicators. These indicators utilize current signal information to provide a real-time assessment of system conditions. By monitoring these health indicators, early signs of damage can be detected, potential failures can be predicted, and proactive maintenance strategies can be implemented. An integrated approach that uses current signals and advanced data processing techniques such as PCA ensures a robust and accurate health monitoring system, thereby increasing the reliability and longevity of monitored equipment. The flow diagram summarizes this methodology, emphasizing a seamless transition from data acquisition to health assessment, ultimately improving maintenance and operational efficiency.

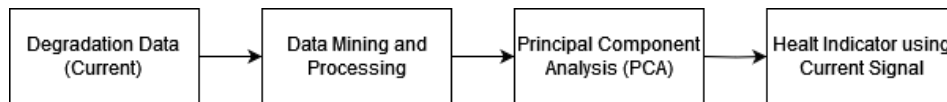


Fig 1. Flow diagram of Health Indicators (HIs) using Principal Component Analysis (PCA)

A. Data Set

The dataset is collected from a three-phase generator. Due to generator coil insulation error, the coil cross-sectional area is decreased, leading to an increase in winding resistance. The synchronous machine block models the machine's electrical part using a sixth-order state-space model for a synchronous generator. This model considers the dynamics of the stator winding, the field, and the damper. The rotor reference frame represents the corresponding circuit, the qd frame, as illustrated in Fig. 2 [15]. The stator windings are connected to the internal neutral point in a wye configuration. All rotor parameters and electrical quantities are analyzed from the stator's reference and identified by their corresponding variables [15].

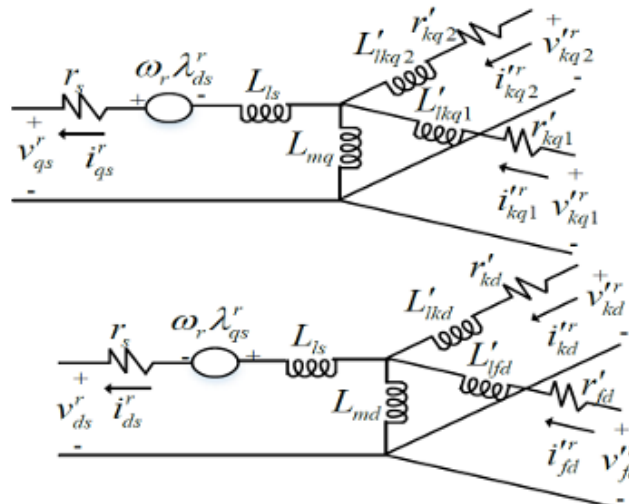


Fig.2. Synchronous Generator Equivalent Model

The state vector consists of the and axis on the stator, axis currents on the stator, the damper winding, and the field winding. The input vector includes the axis voltages on the stator, damper, and field winding. Meanwhile, the output vector comprises the generator output currents on the axes and the excitation current (field current). These relationships are presented in the form of a state-space Equation (1) and (2). The components of matrix A are explained as Equation (3) and (4). The R_{c1} value is presented in Equation (5).

$$\dot{x}(t) = A_c(\omega_r(t))x_c(t) + B_c u_c(t) \tag{1}$$

$$y_c(t) = C_c x_c(t) \tag{2}$$

$$A_c(\omega_r(t)) = (A_{c1} + \omega_r(t)A_{c2}) \tag{3}$$

$$A_{c1} = -L^{-1}R_{c1} = [a_{1ij}]; i, j = 1, \dots, 6 \tag{4}$$

$$R_{c1} = \text{diag}(-r_s, -r_s, r'_{kq1}, r'_{kq2}, \dots, r'_{kq(n_d-1)}, r'_{fd}, r'_{kd}) \tag{5}$$

Considering the state-space model (1), the winding resistance will affect the values of A_{c1} and R_{c1} . Therefore, the effect of reducing the cross-sectional area of the cable roll on the state matrix is defined by equation (7). The complete modelling is detailed as Equation (6) and (7), and the fault vector is defined in Equation (8).

$$A_{cf1} = A_{c1} + F_{c1} \tag{6}$$

$$F_{c1} = -L^{-1} \text{diag}(-r_{dis_s}, -r_{dis_s}, r'_{dis_{kq1}}, r'_{dis_{kq2}}, r'_{dis_{fd}}, r'_{dis_{kd}}) \tag{7}$$

$$f_{c1}(t) = F_{c1}x_c(t) = [f_{1i}(t)]; i = 1, \dots, 6 \tag{8}$$

B. Features Extraction

A portion of the recorded signal is needed for this step to compute many characteristics in the frequency, time, and time-frequency domains. Mechanical vibrations can be effectively analyzed using time and frequency domain analysis techniques [16]. Numerous scholarly publications, conference papers, and technical reports have emphasized the significance of investigations conducted in the time-frequency domain [17]. Indicators that assess signal impulsivity, such as Kurtosis, peak-to-peak value, and peak factor, among others, serve as potential prognostic features for datasets. A clear and detailed description of the feature extraction procedure across these domains is provided.

1) *Time-Domain Feature Extraction:* Time-domain analysis is a straightforward method that mostly concentrates on computing conventional statistical features [16]. This analysis is widely recognized as a powerful tool for characterizing mechanical changes associated with faults [18]. This paper suggests capturing timing information from the data using traditional statistical features, as Table I illustrates. In this context, x represents the sample time signal, the variable i denotes the sample index, and N indicates the total number of samples.

TABLE I
 SUGGESTED TIME-DOMAIN FEATURES

Feature	Expression
RMS	$\left(\frac{1}{N} \sum_{i=1}^N x_i^2\right)^{\frac{1}{2}}$
Kurtosis	$\frac{1}{N} \sum_{i=1}^N \frac{(x_i - \bar{x})^4}{\rho^4}$
Skewness	$\frac{1}{N} \sum_{i=1}^N \frac{(x_i - \bar{x})^3}{\rho^3}$
Peak to peak (P-P)	$x_{max} - x_{min}$
Crest factor	$\frac{x_{max}}{RMS}$
Shape factor	$\frac{RMS}{RMS}$
Impulse factor	$\frac{\frac{1}{N} \sum_{i=1}^N x_i }{x_{max}}$
Margin factor	$\frac{\frac{1}{N} \sum_{i=1}^N x_i }{\left(\frac{1}{N} \sum_{i=1}^N x_i \right)^2}$

Feature	Expression
Mean	$\bar{x} = \frac{1}{N} \sum_{i=1}^N x_i$
Standard deviation (Std)	$\bar{\sigma} = \left(\frac{1}{N} \sum_{i=1}^N (x_i - \text{mean})^2 \right)^{\frac{1}{2}}$
Energy	$\sum_{i=1}^N x_i^2$
Energy entropy	$-\sum_{i=1}^N x_i \log(x_i)$

2) *Frequency-domain feature extraction*: The most widely used technique in the industry for defect diagnosis is frequency domain analysis, which is mainly based on spectral analysis research [16]. In vibration analysis, when a rolling element in a bearing encounters a local defect on its inner or outer race, it creates an impact that induces high-frequency resonances throughout the structure, detectable by response transducers [19]. This method is often employed to observe changes in the frequency spectrum of vibrations or acoustic signals. Using frequency-domain feature extraction, important information within a signal, which may not be readily apparent in time-domain analysis, can be discerned. This approach provides deeper insights into the characteristics and conditions of the signal.

3) *Time-frequency-domain feature extraction*: One popular technique in the literature for obtaining features in the time-frequency domain is Empirical Mode Decomposition (EMD). It has been widely used to identify issues with rotating machinery [17]. EMD breaks down the initial non-stationary vibration signal into stationary signals called intrinsic mode functions (IMFs) [20]. IMFs, naturally occurring oscillation modes included in the signal, are extracted using this self-adaptive signal processing technique [17]. Implementations of EMD lacking a solid theoretical basis may face issues such as tail effects, filtering stopping criteria, and extreme interpolation [21][22]. In this paper, we propose to use time-domain feature extraction methods for several significant reasons:

- a) *Simplicity and Computational Speed*: This method is generally more straightforward and easier to implement than other techniques. Calculations for time-domain feature extraction require fewer computational resources and are faster to process, making them ideal for real-time applications.
- b) *Sensitivity and Anomaly Detection*: Time-domain features are adept at quickly reflecting changes in current signals, enabling rapid detection of changes in conditions. These features also provide direct indications of any anomalies or failures in the signal.
- c) *Practicality in Industrial Applications*: This method is commonly employed in predictive maintenance systems to continuously monitor machine conditions and anticipate maintenance needs before failures occur. It facilitates efficient diagnostics without the complexity of spectral analysis, making it suitable for direct application in industrial settings.

C. Principal Component Analysis

Principal Component Analysis (PCA) is a widely used technique for handling redundant or correlated data in laboratory and process measurements. The relationships between variables and how they alter collectively are frequently where the important insights are found. When characterizing process conditions or events, PCA finds correlations between variables that are more instructive than using just individual variables [23]. PCA is utilized to detect errors and analyze fluctuations in input and output variables within large-scale processes. By decreasing the dimensionality of the dataset, PCA converts correlated variables into a smaller set of uncorrelated variables while preserving essential information [24]. This reduction optimizes the capture of data variance. PCA effectively utilizes redundant information in highly correlated variables, enabling robust detection and diagnosis of process abnormalities after model development using high-quality training data [25].

In Equation (9), the PCA decomposes the data matrix X (consisting of m samples and n variables) as the sum of the outer product of t_i and p_i vectors, along with a residual matrix E [26]. The vectors p_i are orthonormal, and the vectors t_i are orthogonal, as shown in Equation (10). We can also observe that t_i is a linear combination of the original X data, defined by the transformation vector p_i , as indicated in Equation (11).

$$X = t_1 p_1^T + t_2 p_2^T + \dots + t_k p_k^T + E = T_k P_k^T + E \tag{9}$$

$$p_i^T p_j = 1, \text{ if } i = j \text{ and } p_i^T p_j = 0, \text{ if } i \neq j; \text{ and } t_i^T t_j = 0, \text{ if } i \neq j \tag{10}$$

$$X p_i = t_i \tag{11}$$

The vectors represent the principal component scores. t_i r, which illustrates the relationships between the samples. The eigenvectors of matrix X covariance are the p_i vectors. They offer information about the connections between variables, which are primary component loadings. PCA separates the data matrix X PCA into two parts: residual variance E , which captures the noise or unmodeled information, and the system variation, or process $T_k P_k^T$ model.

D. Health Indicator

The choice of thresholds is usually determined by examining historical machine records or leveraging expertise specific to the domain. The health indicator's most recent value was chosen as the threshold because this dataset lacks historical data to lessen the delay impacts of smoothing operations. Thresholds should ideally be based on smoothed previous data. Given the absence of historical data in this dataset, previous slope parameters were arbitrarily selected with high variance ($E(\theta) = 1, Var(\theta) = 10^6, E(\beta) = 1, Var(\beta) = 10^6$) to primarily rely on observed data. Based on $E[h(0)] = \phi + E(\theta)$, intercept ϕ is set to -1 so that the model will start from 0 as well. The relationship between the variation of health indicators and noise variation can be derived using Equation (12).

$$\Delta h(t) \approx (h(t) - \phi)\Delta\epsilon(t) \tag{12}$$

In this case, when the noise standard deviation is near the threshold, it is responsible for a 10% change in the health indicator. Consequently, the noise's standard deviation can be represented as $\frac{10\% \cdot threshold}{threshold - \phi}$.

III. RESULT AND DISCUSSION

A. Data Collection

Based on engine degradation data obtained from the Matlab synchronous simulation data set, the engine in Fig.3, rated 200 MVA, 13.8 kV, 112.5 rpm, is connected to a 230 kV, 10,000 MVA network through a Delta-Wye 210 MVA transformer. The flow measurement time step for the complete dataset is 1 day, with simulations conducted daily for 60 seconds. Current data was collected over 61 days (2 months). Each day's current data included a resistance. R_{c1} added to the simulation, starting at 0.001 on day 1 and increasing linearly to 0.06 by day 61. The overall flow data is illustrated in Fig.4. A slight change in flow was observed in the initial seconds from day 4 to day 62.

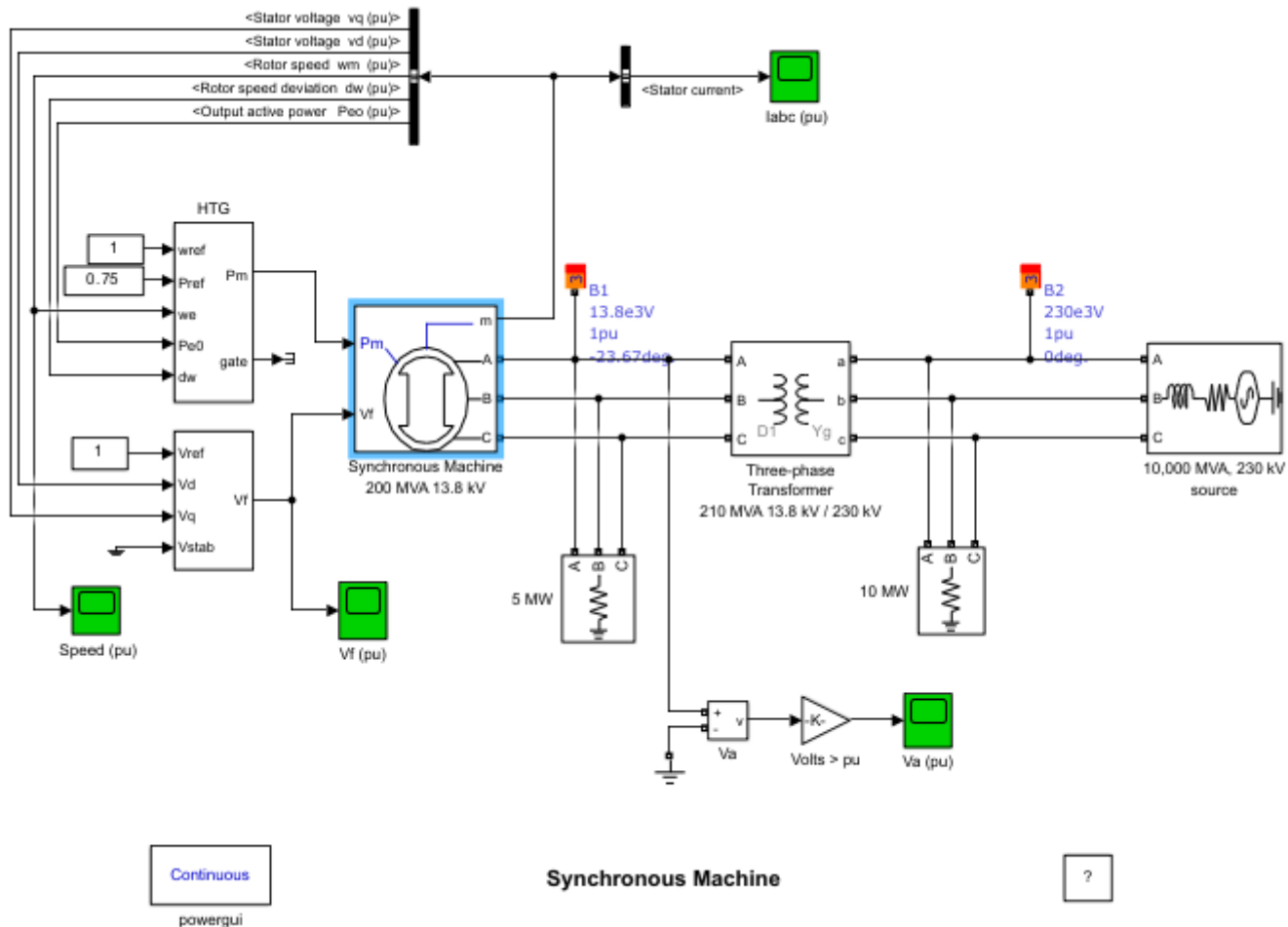


Fig.3. Simulation Three-Phase Generator Synchronous Machine

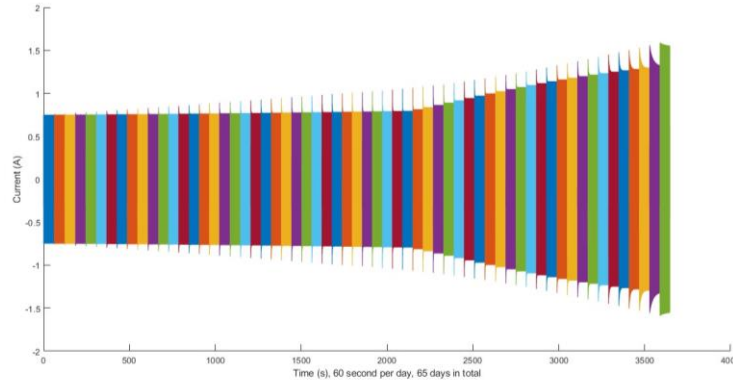


Fig.4. Visualization Of Current Signals in The Time Domain

The error severity level in the colour bar in Fig.5 represents the measurement date normalized to a scale of 0 to 1. It is observed that the spectral kurtosis value around 2000 Amperes gradually increases as the machine condition deteriorates. Statistical features derived from spectral Kurtosis, such as mean and standard deviation, hold promise as potential indicators of bearing degradation.

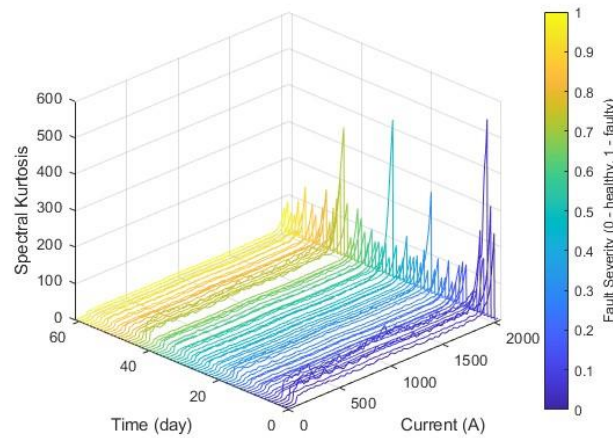


Fig.5. Fault Severity Indicated

B. Feature Extraction

In this research, we investigate the impact of daily changes in R_{c1} resistance, incremented by 0.001, on machine performance and condition monitoring using Principal Component Analysis (PCA). Each day introduces a new value of R_{c1} , and we observe its effects on various extracted features and health indicators. As described earlier in the feature extraction process with equations presented in Table 1, results are plotted in Fig.6, utilizing monotonicity to assess the predictive utility of features. The monotonicity of the i -th feature x_i is computed using Equation (13).

$$Monotonicity(x_i) = \frac{1}{m} \sum_{j=1}^m \frac{|number\ of\ positive\ diff(x_i^j) - number\ of\ negative\ diff(x_i^j)|}{n-1} \tag{13}$$

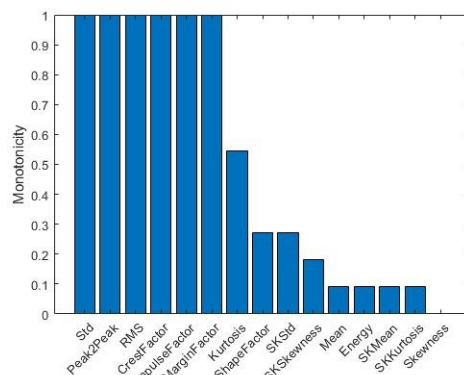


Fig.6. Plot Features Extraction

In practical scenarios, complete life cycle data may not always be available when developing prognostic algorithms. However, it is reasonable to assume that some data has been collected during the early stages of the life cycle. Therefore, the flow data gathered over the first 20 days (40% of the life cycle) is designated training data. The importance of these features is ranked and aggregated based solely on this training data. Features with an importance value greater than 0.3 are selected. Specifically, seven features (Std, Peak to Peak, RMS, Crest factor, Impulse factor, Margin factor, and Kurtosis) meeting this criterion are identified from the training data. This process effectively reduces the dimensionality of the dataset, enhancing the efficiency and accuracy of the model by focusing solely on the most relevant features.

C. PCA & Health Indicator

Principal Component Analysis (PCA) was applied to the extracted features to reduce data dimensionality and identify principal components that best explain variance within the dataset. The first principal component (PCA1) consistently increased with daily increments in resistance, indicating a clear trend corresponding to changes in resistance conditions. Fig.7 visually depicts the results of PCA conducted in this study. The X-axis (PCA 1) represents the primary principal component (PCA1), capturing the most significant variance in the dataset. PCA1 is influenced by key features extracted, such as Std, Peak to Peak, RMS, Crest Factor, Impulse Factor, Margin Factor, and Kurtosis. The Y-axis (PCA 2) represents the second principal component (PCA2), capturing orthogonal variance to PCA1. Each data point is colour-coded to indicate the time of day, progressing from blue (day 1) to yellow (day 61). This visualization effectively illustrates the temporal evolution of data points over the study period.

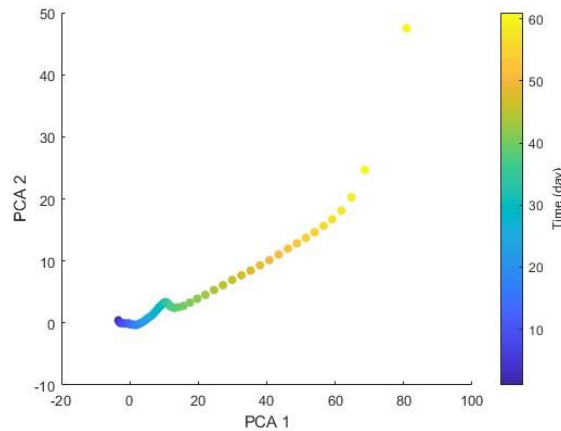
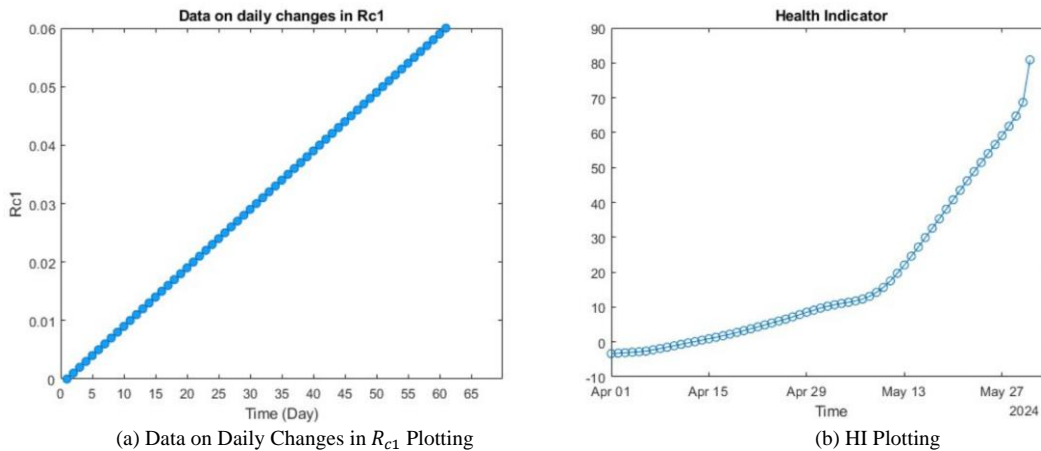


Fig.7. PCA Plotting Simulation Three-Phase Generator Synchronous Machine

In the initial stage (days 1-20), the initial data points (depicted in blue) are clustered near the origin of the PCA space, indicating relatively stable machine conditions with low variance in the extracted features. During the transition stage (days 21-40), the colour gradient shifts from blue to green, showing noticeable trends in the PCA space. There are evident fluctuations in both PCA1 and PCA2 values, suggesting a deteriorating machine condition as resistance levels increase. As the colour transitions from green to yellow, representing the decline phase, data points progressively move upwards and to the right in the PCA plot. This phase is characterized by a significant rise in PCA1 and PCA2 values, indicating substantial degradation of the machine condition. The trend underscores the cumulative impact of resistance changes on engine health. The PCA plot correlates daily resistance variations and the evolving machine condition. Increasing values of PCA1 and PCA2, coupled with the colour shift from blue to yellow, signify a continuous decline in engine health.



(a) Data on Daily Changes in R_{c1} Plotting (b) HI Plotting

Fig.8. Simulation Three-Phase Generator Synchronous Machine HI Curve

The available data and graphs in Fig.8 clearly illustrate the relationship between daily resistance changes (R_{c1}), Principal Component Analysis (PCA) results, and Health Indicators (HIs). Graph (a) demonstrates a linear increase in R_{c1} over time, with a daily increment of 0.001. This controlled rise in resistance is crucial for analyzing machine behaviour and health over an extended period. Graph (b) portrays the trend of HI over time. Initially, HI remains relatively stable at a low level until mid-April. Subsequently, it escalates more rapidly, culminating in a sharp increase by the end of May. By day 61, HI exhibits a significant rise, indicating a pronounced deterioration in machine health.

The PCA plot and HI graph indicate an upward trend as the load increases. This affirms that machine condition worsens under heavier loads, with PCA and HI metrics effectively capturing this degradation. The rapid surge in HI towards the end of the observation period suggests the machine is approaching a critical failure point, consistent with the increasing PCA values.

IV. CONCLUSION

As resistance (R_{c1}) increases linearly over time (t) health indicators also increase, albeit nonlinearly, offering valuable insights for timely intervention before critical failures occur. This analysis reveals a robust correlation between daily incremental changes in resistance and machine condition, as monitored by PCA and health indicators. Consistent upward trends in PCA scores and health indicators affirm the effectiveness of these techniques in monitoring engine health amidst varying resistance levels. Furthermore, current data can be utilized to derive health indicators, with their relationship often following an exponential function. This study underscores the significance of continuous monitoring and applying advanced statistical and signal-processing techniques for predicting and preventing machine failures. The visual representation supports the efficacy of employing PCA and health indicators in predictive maintenance, facilitating proactive interventions before critical failures emerge.

REFERENCES

- [1] R. Khelif, B. Chebel-Morello, S. Malinowski, E. Laajili, F. Fnaiech, and N. Zerhouni, "Direct Remaining Useful Life Estimation Based on Support Vector Regression," *IEEE Trans. Ind. Electron.*, vol. 64, no. 3, pp. 2276–2285, 2017, doi: 10.1109/TIE.2016.2623260.
- [2] E. Zio, "Some Challenges and Opportunities in Reliability Engineering," *IEEE Trans. Reliab.*, vol. 65, no. 4, pp. 1769–1782, 2016, doi: 10.1109/TR.2016.2591504.
- [3] T. Chen, T. Feng, Y. Yu, L. Guo, H. Gao, and W. Lfi, "Adaptive weighted fault growth parameters: New statistic parameter health indicators for machine performance degradation assessment," *Measurement*, vol. 216, p. 112830, 2023, doi: <https://doi.org/10.1016/j.measurement.2023.112830>.
- [4] J. Pan *et al.*, "Probabilistic remaining useful life prediction without lifetime labels: A Bayesian deep learning and stochastic process fusion method," *Reliab. Eng. Syst. Saf.*, p. 110313, 2024, doi: <https://doi.org/10.1016/j.res.2024.110313>.
- [5] L. Guo, Y. Yu, A. Duan, H. Gao, and J. Zhang, "An unsupervised feature learning based health indicator construction method for performance assessment of machines," *Mech. Syst. Signal Process.*, vol. 167, p. 108573, 2022, doi: <https://doi.org/10.1016/j.ymsp.2021.108573>.
- [6] Q. Ni, J. C. Ji, and K. Feng, "Data-Driven Prognostic Scheme for Bearings Based on a Novel Health Indicator and Gated Recurrent Unit Network," *IEEE Trans. Ind. Informatics*, vol. 19, no. 2, pp. 1301–1311, 2023, doi: 10.1109/TII.2022.3169465.
- [7] Y.-S. Zhao, P. Li, Y. Kang, and Y.-B. Zhao, "A health indicator enabling both first predicting time detection and remaining useful life prediction: Application to rotating machinery," *Measurement*, vol. 235, p. 114994, 2024, doi: <https://doi.org/10.1016/j.measurement.2024.114994>.
- [8] Y. Lei, N. Li, L. Guo, N. Li, T. Yan, and J. Lin, "Machinery health prognostics: A systematic review from data acquisition to RUL prediction," *Mech. Syst. Signal Process.*, vol. 104, pp. 799–834, 2018, doi: <https://doi.org/10.1016/j.ymsp.2017.11.016>.
- [9] A. Aasi, R. Tabatabaei, E. Aasi, and S. M. Jafari, "Experimental investigation on time-domain features in the diagnosis of rolling element bearings by acoustic emission," *J. Vib. Control*, vol. 28, no. 19–20, pp. 2585–2595, 2022, doi: 10.1177/10775463211016130.
- [10] T. Yan, D. Wang, B. Hou, and Z. Peng, "Generic Framework for Integration of First Prediction Time Detection With Machine Degradation Modelling from Frequency Domain," *IEEE Trans. Reliab.*, vol. 71, no. 4, pp. 1464–1476, 2022, doi: 10.1109/TR.2021.3087698.
- [11] Y. Duan, X. Cao, J. Zhao, and X. Xu, "Health indicator construction and status assessment of rotating machinery by spatio-temporal fusion of multi-domain mixed features," *Measurement*, vol. 205, p. 112170, 2022, doi: <https://doi.org/10.1016/j.measurement.2022.112170>.
- [12] Q. Ni, J. C. Ji, K. Feng, and B. Halkon, "A fault information-guided variational mode decomposition (FIVMD) method for rolling element bearings diagnosis," *Mech. Syst. Signal Process.*, vol. 164, p. 108216, 2022, doi: <https://doi.org/10.1016/j.ymsp.2021.108216>.
- [13] J. Coble and J. Wesley Hines, "Identifying optimal prognostic parameters from data: A genetic algorithms approach," *Annu. Conf. Progn. Heal. Manag. Soc. PHM 2009*, pp. 1–11, 2009.
- [14] G. Zhang, Y. Wang, X. Li, Y. Qin, and B. Tang, "Health indicator based on signal probability distribution measures for

- machinery condition monitoring," *Mech. Syst. Signal Process.*, vol. 198, p. 110460, 2023, doi: <https://doi.org/10.1016/j.ymsp.2023.110460>.
- [15] Z. Masoumi, B. Moaveni, S. M. Mousavi Gazafrudi, and J. Faiz, "Air-gap eccentricity fault detection, isolation, and estimation for synchronous generators based on eigenvalues analysis," *ISA Trans.*, vol. 131, pp. 489–500, 2022, doi: <https://doi.org/10.1016/j.isatra.2022.04.038>.
- [16] N. Tandon and A. Choudhury, "A review of vibration and acoustic measurement methods for the detection of defects in rolling element bearings," *Tribol. Int.*, vol. 32, no. 8, pp. 469–480, 1999, doi: [https://doi.org/10.1016/S0301-679X\(99\)00077-8](https://doi.org/10.1016/S0301-679X(99)00077-8).
- [17] Y. Lei, J. Lin, Z. He, and M. J. Zuo, "A review on empirical mode decomposition in fault diagnosis of rotating machinery," *Mech. Syst. Signal Process.*, vol. 35, no. 1, pp. 108–126, 2013, doi: <https://doi.org/10.1016/j.ymsp.2012.09.015>.
- [18] J. Ben Ali, N. Fnaiech, L. Saidi, B. Chebel-Morello, and F. Fnaiech, "Application of empirical mode decomposition and artificial neural network for automatic bearing fault diagnosis based on vibration signals," *Appl. Acoust.*, vol. 89, pp. 16–27, 2015, doi: <https://doi.org/10.1016/j.apacoust.2014.08.016>.
- [19] J. Ben Ali, B. Chebel-Morello, L. Saidi, S. Malinowski, and F. Fnaiech, "Accurate bearing remaining useful life prediction based on Weibull distribution and artificial neural network," *Mech. Syst. Signal Process.*, vol. 56–57, pp. 150–172, 2015, doi: <https://doi.org/10.1016/j.ymsp.2014.10.014>.
- [20] L. Saidi, J. Ben Ali, and F. Fnaiech, "Bi-spectrum based-EMD applied to the non-stationary vibration signals for bearing faults diagnosis," *ISA Trans.*, vol. 53, no. 5, pp. 1650–1660, 2014, doi: <https://doi.org/10.1016/j.isatra.2014.06.002>.
- [21] R. T. Rato, M. D. Ortigueira, and A. G. Batista, "On the HHT, its problems, and some solutions," *Mech. Syst. Signal Process.*, vol. 22, no. 6, pp. 1374–1394, 2008, doi: <https://doi.org/10.1016/j.ymsp.2007.11.028>.
- [22] G. Chen and Z. Wang, "A signal decomposition theorem with Hilbert transform and its application to narrowband time series with closely spaced frequency components," *Mech. Syst. Signal Process.*, vol. 28, pp. 258–279, 2012, doi: <https://doi.org/10.1016/j.ymsp.2011.02.002>.
- [23] S. Li and J. Wen, "A model-based fault detection and diagnostic methodology based on PCA method and wavelet transform," *Energy Build.*, vol. 68, pp. 63–71, 2014, doi: <https://doi.org/10.1016/j.enbuild.2013.08.044>.
- [24] A. Ajami and M. Daneshvar, "Data driven approach for fault detection and diagnosis of turbine in thermal power plant using Independent Component Analysis (ICA)," *Int. J. Electr. Power Energy Syst.*, vol. 43, no. 1, pp. 728–735, 2012, doi: <https://doi.org/10.1016/j.ijepes.2012.06.022>.
- [25] R. Penha and J. W. Hines, "Using principal component analysis modeling to monitor temperature sensors in a nuclear research reactor," 2001.
- [26] N. B. Gallagher, B. M. Wise, S. W. Butler, D. D. White, and G. G. Barna, "Development and Benchmarking of Multivariate Statistical Process Control Tools for a Semiconductor Etch Process: Improving Robustness through Model Updating," *IFAC Proc. Vol.*, vol. 30, no. 9, pp. 79–84, 1997, doi: [https://doi.org/10.1016/S1474-6670\(17\)43143-0](https://doi.org/10.1016/S1474-6670(17)43143-0).